

Synthesis and Properties of Terthiophene and Bithiophene Derivatives Functionalized by BF₂ Chelation: A New Type of Electron Acceptor Based on Quadrupolar Structures

Katsuhiko Ono,*^[a] Akihiro Nakashima,^[a] Yujiro Tsuji,^[a] Takatoshi Kinoshita,^[a] Masaaki Tomura,^[b] Jun-ichi Nishida,^[c] and Yoshiro Yamashita^[c]

Abstract: Terthiophene and bithiophene derivatives functionalized by BF₂ chelation were synthesized as a new type of electron acceptor, and their properties were compared to those of bifuran and biphenyl derivatives. These new compounds are characterized by quadrupolar structures due to resonance contributors generated by BF₂ chelation. The bithiophene derivative has a strong quadrupolar character compared with the bifuran and biphenyl derivatives because their

hydrolytic analyses indicated that the bithiophene moiety has a larger on-site Coulomb repulsion than the others. The terthiophene derivative has a smaller on-site Coulomb repulsion than the bithiophene derivative due to the addition of a thiophene spacer. These BF₂ complexes exhibit long-wavelength

absorptions and according to measurements of ionization potentials and absorption edges they have energetically low-lying HOMOs and LUMOs. The crystal structure of the bithiophene derivative is of the herringbone type, with short F...S and F...C contacts affording dense crystal packing. n-Type semiconducting behaviour was observed in organic field-effect transistors based on these BF₂ complexes.

Keywords: boron • chelates • electron-deficient compounds • heterocycles • semiconductors

Introduction

Boron complexes are highly attractive targets in the research and development of materials for organic devices because they have pronounced electron-accepting properties and strong fluorescence with high quantum yields. Their properties vary depending on the ligand structures and substituents on the boron atoms. Boron complexes with aromat-

ic heterocyclic ligands, such as 2-(2-hydroxyphenyl)pyridines,^[1] 2-(2-pyridyl)indoles,^[2] and 2-(2-pyrrolyl)quinolines,^[3] were applied as fluorescent emitters in studies on organic light-emitting diodes (OLEDs). Organoboron quinolates with various functional groups were also synthesized and their electro- and photoluminescence properties were studied.^[4] These units were integrated into polymers to produce light-emitting materials.^[5] The known boradiazaindacene (BODIPY) fluorophores are used as light-sensing units and fluorescent probes in sensor materials.^[6–8] In particular, they have been studied as electron-accepting units of photoinduced charge-transfer materials for application in dye-sensitized solar cells (DSCs).^[9] Recently, boron complexes with subporphyrins were synthesized and their optical properties investigated.^[10]

Boron diketonates have also attracted considerable attention as fluorophores and electron-accepting units.^[11–16] Among these compounds, difluoroboron complexes have been synthesized as potential electron-transporting materials. For example, a BF₂ complex with 1,6-diphenyl-1,3,4,6-hexanetetron exhibited n-type semiconducting behaviour in organic field-effect transistors (OFETs).^[15] Recently, we reported the n-type semiconducting properties of BF₂ com-

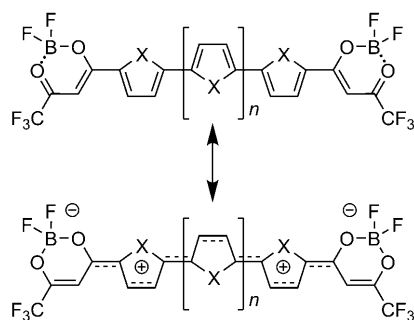
[a] Prof. Dr. K. Ono, A. Nakashima, Y. Tsuji, Prof. Dr. T. Kinoshita
Graduate School of Engineering
Nagoya Institute of Technology
Gokiso, Showa-ku, Nagoya 466-8555 (Japan)
Fax: (+81)52-735-5407
E-mail: ono.katsuhiko@nitech.ac.jp

[b] Dr. M. Tomura
Institute for Molecular Science
Myodaiji, Okazaki 444-8585 (Japan)

[c] Dr. J.-i. Nishida, Prof. Dr. Y. Yamashita
Interdisciplinary Graduate School of Science and Engineering
Tokyo Institute of Technology
Nagatsuta, Midori-ku, Yokohama 226-8502 (Japan)

Supporting information for this article is available on the WWW under <http://dx.doi.org/10.1002/chem.201001185>.

plexes with 6,11-dihydroxy-5,12-naphthacenediones (DHNDs) as a new type of electron-deficient acene compounds.^[16] Chelation of BF₂ enhanced the electron affinity and π -electron delocalization of the tetracene moieties. To investigate π -conjugated systems functionalized by BF₂ chelation, we synthesized terthiophene **1a** and bithiophene **1b** with two difluoroboron diketonate units, as well as bifuran derivative **1c** and biphenyl derivative **1d** (Scheme 1) be-



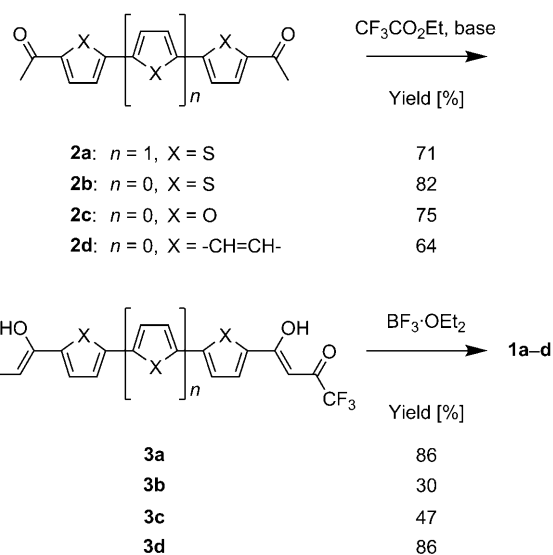
- 1a:** $n = 1, X = S$
1b: $n = 0, X = S$
1c: $n = 0, X = O$
1d: $n = 0, X = -CH=CH-$

Scheme 1. Structure of BF₂ complexes **1** with quadrupolar contributions, in which two negative charges are localized on the boron atoms and two positive charges are delocalized over the arylene moieties.

cause various electron-deficient compounds with oligothiophene skeletons are of interest as n-type semiconductors in OFETs.^[17] These compounds have quadrupolar character, as represented by the resonance contributors generated by BF₂ chelation. Thus, arylene moieties such as terthiophene and bithiophene become electron-deficient π -electron systems. When the π -conjugated systems have a larger on-site Coulomb repulsion, the difluoroboron diketonates become unstable. We studied the instability of BF₂ chelation by using hydrolytic analysis. Furthermore, molecular arrangements of BF₂ complexes in the crystal have attracted considerable attention because they form dense crystal packings with short heteroatom contacts.^[11,14,16b] Herein we report the synthesis, electron-accepting properties and crystal structure of BF₂ complexes **1** and their application to OFETs.

Results and Discussion

Synthesis and stability of BF₂ complexes: The synthesis of BF₂ complexes **1** is illustrated in Scheme 2. Diacetyl compounds **2a–d** reacted with ethyl trifluoroacetate in the presence of lithium bis(trimethylsilyl)amide or NaOMe to afford ligands **3** in 64–82% yields. BF₂ complexes **1** were synthesized by treatment of ligands **3a–d** with BF₃·OEt₂. Compound **1a** was obtained as dark purple crystals in 86% yield after removal of excess BF₃·OEt₂ and washing with chloro-



Scheme 2. Synthesis of BF₂ complexes **1**.

form and *n*-hexane. Compounds **1b–d** were prepared as red, orange and yellow crystals, respectively, in 30–86% yield after sublimation. Their structures were determined by means of spectral data and elemental analyses. Compounds **1** were immediately hydrolyzed in solution to afford ligands **3**, whereas they were relatively stable in dry acetonitrile, chloroform and dichloromethane. In the solid state, compounds **1** were stable in air. The stability of **1** in the presence of moisture is considerably higher than that of the BF₂ complex of 1,4-phenylene, which decomposed in air within a day, even in the solid state. Compounds **1** were thermally stable under inert atmosphere. Thermogravimetry (TG) measurements on **1** revealed thermal stability up to 200°C; 5% weight loss was observed at 261, 253, 236 and 235°C for **1a–d**, respectively.

Spectroscopic properties of BF₂ complexes: The UV/Vis absorption spectra of **1** were measured in acetonitrile (Figure 1). The red-shifted absorption maxima (Table 1) compared with ligands **3** ($\lambda_{\max} = 453, 421, 412$ and 362 nm for

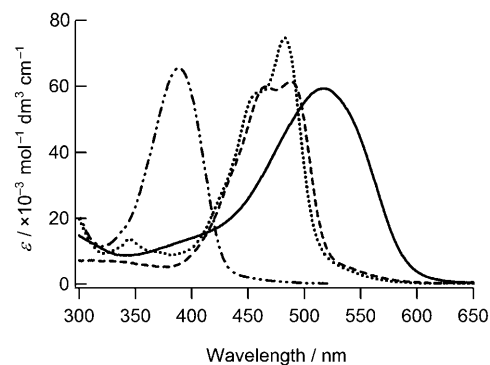


Figure 1. UV/Vis absorption spectra of BF₂ complexes **1** in acetonitrile; —: **1a**, ---: **1b**,: **1c**, -·-·-: **1d**.

Table 1. UV/Vis absorption and fluorescence properties of BF₂ complexes **1**.^[a]

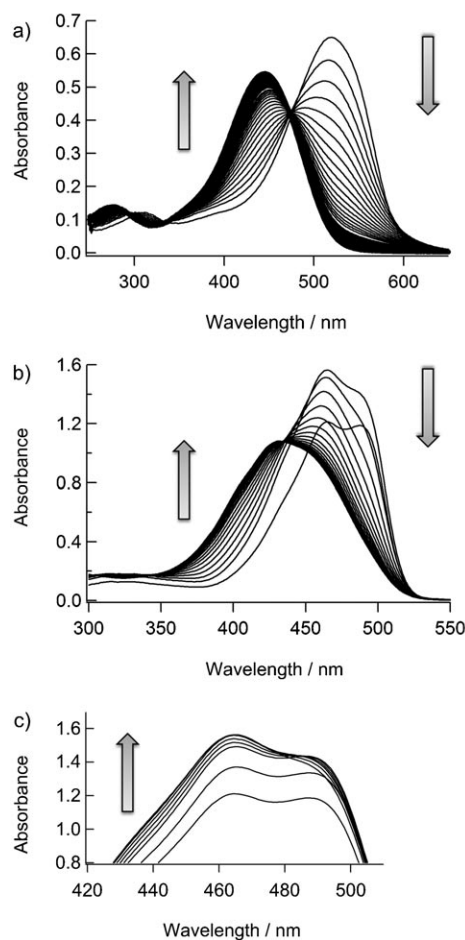
	λ_{abs} [nm] (ϵ [mol ⁻¹ dm ³ cm ⁻¹])	E_{gap} [eV] ^[b]	λ_{em} [nm]
1a	517 (59 400)	2.09	608
1b	488 (61 500), 466 (59 900)	2.38	518
1c	482 (74 800), 457 sh (57 900)	2.42	516
1d	389 (65 500)	2.89	448

[a] In acetonitrile. [b] Estimated from the absorption edge.

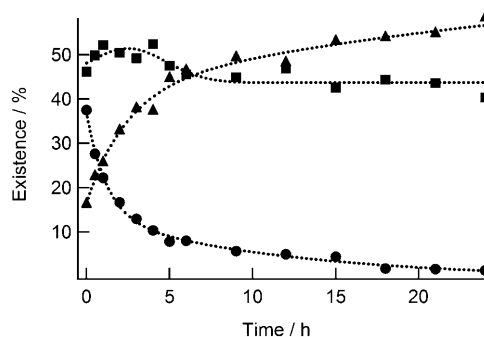
3a, **3b**, **3c** and **3d**, respectively) indicate significant contributions of quadrupolar structures generated by BF₂ chelation (Scheme 1). The absorption maximum of **1a** is red-shifted by about 30 nm relative to **1b,c**, which are red-shifted by about 100 nm in comparison to **1d**. This indicates that the shift of the absorption bands depends on the arylene moieties linking the two difluoroboron diketonate units. The maximum molar absorption coefficients of **1a–d** lie in a similar range. The absorption maximum of **1a** is red-shifted by 165 nm compared to that of terthiophene ($\lambda_{\text{max}}=352$ nm) and the molar absorption coefficient of **1a** is three times larger than that of terthiophene ($\epsilon=19\,500$ mol⁻¹dm³cm⁻¹; Figure S4 in the Supporting Information). This indicates extension of the π -electron system in **1a** by introduction of the difluoroboron diketonate moieties. Furthermore, the broad absorption band of **1a** is due to the terthiophene skeleton. When the number of thiophene rings increased, the band shape became broader and longer wavelength absorption edges resulted. The HOMO–LUMO energy gaps (E_{gap}) for **1a–d** were found to be in the range of 2.09–2.89 eV (Table 1).

Boron complexes **1** exhibit photoluminescence (PL) in solution; emission maxima are listed in Table 1. The Stokes shifts of **1a–d** of 30–91 nm are larger than that of DHND–BF₂ (6 nm),^[16] that is, compounds **1** have flexible geometries. Only compound **1d** exhibited PL in the solid state, and its emission maximum ($\lambda_{\text{max}}=519$ nm) was red-shifted by 71 nm compared to that observed in solution.

Intramolecular interaction between the two difluoroboron diketonate moieties: To investigate intramolecular interactions between the two difluoroboron diketonate moieties, we studied hydrolysis of **1** in acetonitrile. The UV/Vis absorption spectra of **1a** were monitored as a function of time over 3 d (Figure 2a). The maximum absorption intensity at $\lambda=517$ nm gradually decreased and an absorption band due to ligand **3a** emerged. This decay consisted of two types of reaction with first-order kinetics (Figure S6a in the Supporting Information). The fast reaction is hydrolysis of **1a** to generate a metastable mono-BF₂ complex with a rate constant of $k_1=5.0\times 10^{-5}$ s⁻¹, measured over the period of 0–16 h. The slow reaction is hydrolysis of the mono-BF₂ complex to give ligand **3a** with a rate constant of $k_2=1.7\times 10^{-5}$ s⁻¹, obtained over the period of 22–67 h. Thus, the first step of the hydrolysis proceeded three times faster than the second step. Hydrolysis of **1a** was also monitored by time-dependent ¹H NMR spectroscopy in [D₃]acetonitrile (Fig-

Figure 2. Time-dependent absorption spectra of a) **1a** ($c=1.1\times 10^{-5}$ M) and b) **1b** ($c=2.0\times 10^{-5}$ M) in acetonitrile at 1 h intervals and c) **1b** at 10 min intervals for the initial 70 min.

ure S9a in the Supporting Information). The ratio of **1a**, mono-BF₂ complex and ligand **3a** as a function of time (Figure 3) indicates that **1a** was consumed primarily over the period of 0–20 h. This rate constant k_1 for the hydrolysis of **1a** to give the mono-BF₂ complex was determined to be 8.2×10^{-5} s⁻¹ (Figure S9b in the Supporting Information),

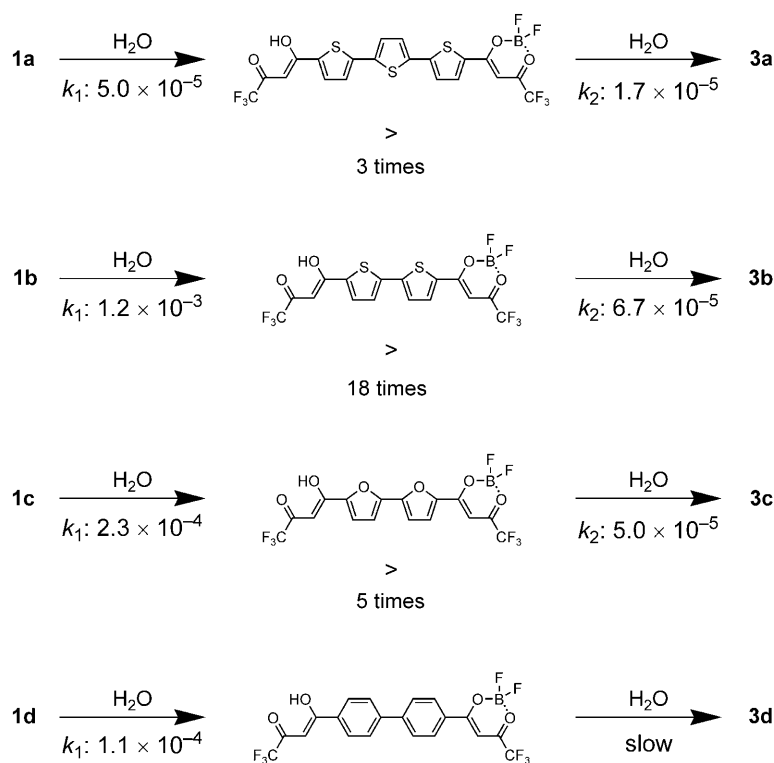
Figure 3. Progress in the hydrolysis of **1a** monitored by time-dependent ¹H NMR spectra in [D₃]acetonitrile: **1a** (●), mono-BF₂ complex (■) and ligand **3a** (▲).

which is similar to the k_1 value measured by analysis of the UV/Vis absorption spectrum.

The hydrolysis of **1b** was also elucidated by analysis of the UV/Vis absorption spectrum (Figure 2b and c). For the initial 40 min, the intensity of the absorption maximum at $\lambda = 466$ nm increased (Figure 2c) and thus indicated generation of a mono-BF₂ complex. After that, the intensity of the absorption bands gradually decreased with an isobestic point, and the spectrum of ligand **3b** resulted (Figure 2b). This spectral change indicates that the hydrolysis of **1b** generating its mono-BF₂ complex is much faster than that of the mono-BF₂ complex to give ligand **3b**. The k_1 and k_2 values were found to be 1.2×10^{-3} and $6.7 \times 10^{-5} \text{ s}^{-1}$, respectively (Figure S6b in the Supporting Information).

The time-dependent absorption spectra of **1c** and **1d** are shown in Figure S7 and S8 in the Supporting Information, respectively. In the hydrolysis of **1c**, we observed an increase in absorbance in the initial stage and then gradual decay of the absorption bands, resulting in the spectrum of ligand **3c**. This spectral change is similar to that of **1b**. On the other hand, the hydrolysis of **1d** exhibited a spectral change similar to that of **1a**. Thus, the spectral changes depended on the nature of the arylene moieties. Complexes **1a** and **1d** exhibited a single absorption maximum, whereas **1b** and **1c** revealed two absorption maxima (Table 1). These absorption properties may be responsible for the differences in spectral changes.

Scheme 3 summarizes the rate constants (k_1 and k_2) for the hydrolysis of **1**. The k_1 values of **1c,d** were similar to each other and smaller than that of **1b**. This suggests that **1b** has a larger on-site Coulomb repulsion on the bithiophene moiety, which indicates a significant contribution of the quadrupolar structure (Scheme 1). Thus, the k_1 value of **1b** was 18 times greater than the k_2 value. Furthermore, the k_1 value of **1a** was smaller than those of **1b-d**, that is, **1a** has a smaller on-site Coulomb repulsion than **1b** due to the longer distance between the difluoroboron diketonate moieties because of the additional thiophene spacer. Thus, the hydrolytic analysis indicates that the two difluoroboron diketonate units interact with each other through the linking arylene moieties.



Scheme 3. First-order rate constants [s^{-1}] for the hydrolysis of **1** in acetonitrile from time-dependent absorption spectral analysis.

Electron-accepting properties of BF₂ complexes: To investigate the electron affinities of **1**, cyclic voltammetry (CV) measurements were performed. However, the reproducibility of reduction waves was poor because of the instability of **1** in solution. The ionization potentials of **1b-d** were measured in air by using a photoelectron spectrometer (Riken Keiki AC-3), and their HOMO energy levels were determined to be -6.55 (**1b**), -6.50 (**1c**) and -6.56 eV (**1d**). According to their absorption band edges (Table 1), their LUMO energy levels were estimated to be -4.17 (**1b**), -4.08 (**1c**) and -3.67 eV (**1d**). These LUMO energies are comparable to those of α,ω -diperfluorohexylquaterthiophene (DFH-4T, -3.31 eV) and 5,5'''-diperfluorohexylcarbonyl-2,2':5',2'':5'',2''':5''',2''''-quaterthiophene (DFHCO-4T, -3.96 eV)^[17a,b] and indicate that compounds **1** have strong electron-accepting abilities.

Molecular orbital (MO) calculations on **1** were performed at the B3LYP/6-31G(d) level,^[18] and the energy diagram of their HOMOs and LUMOs is summarized in Figure 4. The energy diagram supports the experimental data for **1b-d**. The HOMO and LUMO energies of **1a** are higher than those of **1b** due to addition of a thiophene spacer. The HOMO-LUMO energy gap of **1a** is smaller than that of **1b**, because of the extended π conjugation of the thiophene moiety. The HOMOs and LUMOs of **1a,b** are attributed to the aromatic and quadrupolar structures of their resonance contributors, respectively (Figure S11 in the Supporting In-

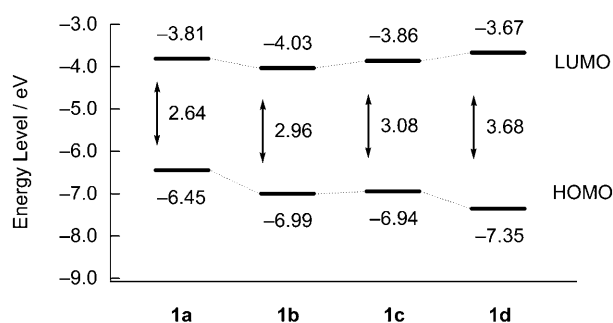


Figure 4. Energy diagram of the HOMOs and LUMOs of BF₂ complexes **1** obtained from B3LYP/6-31G(d) calculations; values given in eV.

formation). The MOs exist on the whole thiophene moieties, that is, compounds **1a,b** are effective π -conjugated systems.

X-ray crystallographic analysis of BF₂ complex: The molecular and crystal structures of **1b** were investigated by X-ray crystallographic analysis. Single crystals suitable for X-ray analysis were grown by slow sublimation at 160 °C under nitrogen. The molecular structure is shown in Figure 5a. Six-membered rings containing boron atoms were found and B–O distances in the range of 1.46–1.53 Å were observed. These rings are almost planar and coplanar with the neigh-

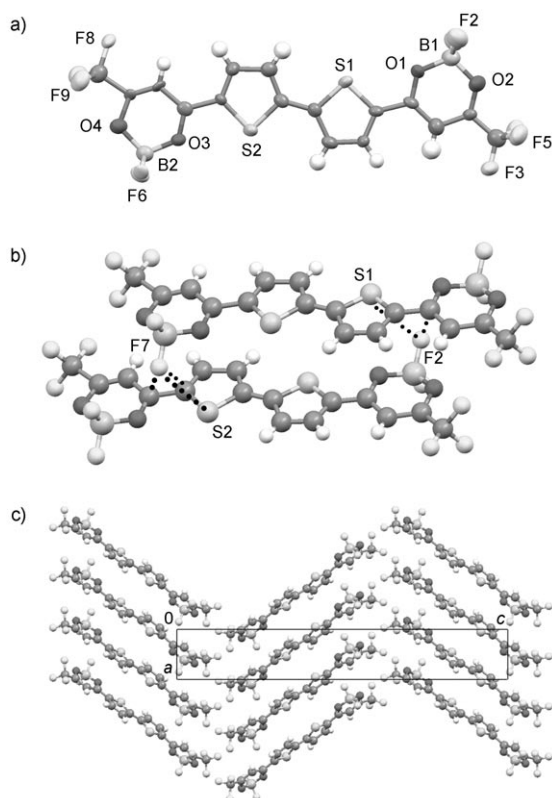


Figure 5. X-ray crystallographic analysis of **1b**: a) molecular structure (ellipsoids were drawn at the 50% probability level), b) overlap mode, c) crystal structure.

boring bithiophene moiety. The B–F bonds are almost symmetrically located on the molecular plane. The molecules are stacked into a columnar structure in an overlap mode that decreases steric hindrance (Figure 5b). The face-to-face stacking is induced by short F...S (3.15 and 3.22 Å) and F...C (3.11–3.14 Å) contacts, which are shorter than the sum of the van der Waals radii (F...S 3.27, F...C 3.17 Å). The crystal structure is of the herringbone type (Figure 5c). The molecular sheets interact with each other through short C–H...F contacts to form a three-dimensional (3D) network. These heteroatom contacts result in dense packing in the crystal ($\rho_{\text{calcd}} = 1.86 \text{ g cm}^{-3}$).

n-Type semiconducting properties of BF₂ complexes: Field-effect mobilities were measured on OFET devices with a bottom-contact configuration. The organic layers were formed on SiO₂ dielectric layers by vacuum deposition (10^{-5} Pa) and the measurements were performed in vacuum. The OFET devices with the films of **1b–d** exhibited n-type semiconducting behaviour with electron mobilities of $6.3 \times 10^{-5} \text{ (1b)}$, $1.2 \times 10^{-6} \text{ (1c)}$ and $7.0 \times 10^{-5} \text{ cm}^2 \text{ V}^{-1} \text{ s}^{-1} \text{ (1d)}$, whereas p-type semiconducting behaviour was not observed because these complexes have low HOMO energies. Thus, these BF₂ complexes are useful as electron acceptors in OFET devices. Therefore, we synthesized BF₂ complex **1e**, in which perfluorohexyl groups are introduced to improve the molecular assembly in an OFET film. Relatively good n-type semiconducting behaviour was observed in a film of **1e** deposited on a hexamethyldisilazane (HMDS)-treated SiO₂ substrate at 90 °C. The output and transfer characteristics are shown in Figure 6. The electron mobility and on/off ratio were calculated to be $2.0 \times 10^{-3} \text{ cm}^2 \text{ V}^{-1} \text{ s}^{-1}$ and 1.0×10^6 , respectively.^[19] The device also exhibited n-type semiconducting behaviour in air and in vacuum in the gate voltage region of 10–40 V. Further modification of **1e** by lower-

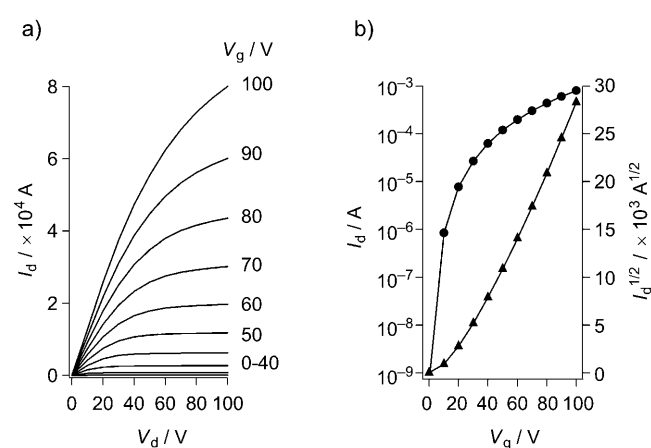
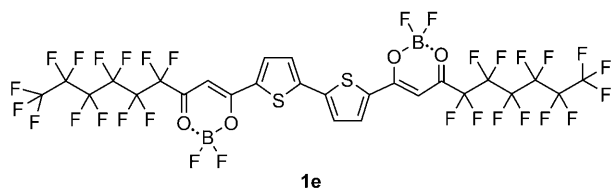


Figure 6. a) Drain current (I_d) vs. drain voltage (V_d) as a function of gate voltage (V_g) for a bottom-contact OFET with **1e** deposited on a HMDS-treated SiO₂ substrate at 90 °C. b) I_d (●) and $I_d^{1/2}$ (▲) vs. V_g plots at $V_d = 100 \text{ V}$ for the same device. The field-effect mobility calculated in the saturation regime is $2.0 \times 10^{-3} \text{ cm}^2 \text{ V}^{-1} \text{ s}^{-1}$.

ing its LUMO energy is expected to give an air-stable n-type OFET.



Conclusion

We have synthesized terthiophene and bithiophene derivatives functionalized by BF₂ chelation as well as bifuran and biphenyl derivatives. These compounds have quadrupolar structures due to their resonance contributors generated by BF₂ chelation. The bithiophene derivative has a stronger quadrupolar character than the bifuran and biphenyl derivatives because it has a larger on-site Coulomb repulsion according to hydrolytic analysis. The on-site Coulomb repulsion of the terthiophene derivative was smaller than that of the bithiophene derivative. These BF₂ complexes exhibited long-wavelength absorptions and low-lying HOMOs and LUMOs, as revealed by the spectroscopic studies and MO calculations. The crystal structure of the bithiophene derivative is of the herringbone-type with short F...S and F...C contacts that result in a 3D network. n-Type semiconducting behaviour was observed in OFET devices based on films of the BF₂ complexes. Notably, a bithiophene derivative with perfluorohexyl groups exhibited relatively high n-type semiconductor performance. Thus, BF₂ functionalization of oligothiophenes gives a new type of electron acceptor that is useful for application in OFETs.

Experimental Section

General: Melting points were measured by using a Yanaco micro melting point apparatus and are uncorrected. ¹H NMR spectra were recorded by using a Bruker Avance 600 spectrometer (600 MHz). IR, UV/Vis and PL spectra were obtained by using Jasco FT/IR-5300, Hitachi U-3500 and Otsuka Electronics PFI-5100S spectrometers, respectively. Mass spectra (EI) were determined by using a Hitachi M-2000S mass spectrometer. Elemental analyses were performed by using a Perkin-Elmer 2400II analyzer. Compounds **2a–c** were synthesized by procedures reported in the literature (see the Supporting Information). Compound **2d** was purchased from Wako Pure Chemical Industries.

Synthesis of ligand 3a: Lithium bis(trimethylsilyl)amide in THF (1.6 M, 2.0 mL, 3.2 mmol) was added dropwise to a solution of 5,5'-diacetyl-2,2':5',2''-terthiophene (**2a**)^[20] (0.40 g, 1.2 mmol) in dry THF (30 mL) at 0°C under nitrogen. Ethyl trifluoroacetate (0.40 mL, 3.4 mmol) was added dropwise to the solution and the mixture was stirred at 0°C for 30 min and at RT overnight. The reaction mixture was treated with hydrochloric acid (2 M, 10 mL) and ethyl acetate (20 mL) was added. The organic layer was separated, then the solution washed with water (20 mL × 3) and dried over Na₂SO₄. After removal of the solvent, the residue was filtered and washed with *n*-hexane to afford a red solid (0.67 g). The crude product was purified by sublimation at 190°C under 10⁻³ Torr

to provide ligand **3a** as dark red crystals (0.45 g, 71%). M.p. 196–197°C; ¹H NMR (600 MHz, CDCl₃): δ = 6.42 (s, 2H), 7.28 (d, *J* = 4.1 Hz, 2H), 7.33 (s, 2H), 7.75 ppm (d, *J* = 4.1 Hz, 2H); IR (KBr): $\tilde{\nu}$ = 1578, 1435, 1424, 1281, 1271, 1246, 1194, 1150, 1113, 1076, 795 cm⁻¹; UV/Vis (MeCN): λ_{max} (ϵ) = 453 nm (56 200 mol⁻¹ dm³ cm⁻¹); MS (70 eV): *m/z* (%): 524 (100) [M]⁺, 455 (37); elemental analysis calcd (%) for C₂₀H₁₀F₆O₄S₃: C 45.80, H 1.92; found: C 46.04, H 1.64.

Ligand 3e: Obtained as yellow crystals (0.65 g, 86%). M.p. 207–208°C; ¹H NMR (600 MHz, CDCl₃): δ = 6.47 (s, 2H), 7.40 (d, *J* = 4.1 Hz, 2H), 7.79 ppm (d, *J* = 4.1 Hz, 2H); IR (KBr): $\tilde{\nu}$ = 1632, 1572, 1302, 1235, 1198, 1144, 793, 725 cm⁻¹; UV/Vis (CH₂Cl₂): λ_{max} (ϵ) = 430 nm (44 400 mol⁻¹ dm³ cm⁻¹); MS (70 eV): *m/z* (%): 944 (82) [M+2]⁺, 623 (100); elemental analysis calcd (%) for C₂₆H₈F₂₆O₄S₂: C 33.14, H 0.86; found: C 33.17, H 0.92.

Ligands 3b–d: Similar reaction conditions were applied but with NaOMe as a base. Ethyl trifluoroacetate (4.0 mL, 34 mmol) was added dropwise to a solution of NaOMe (Na 0.40 g, 17 mmol) in dry methanol (10 mL) and dry diethyl ether (20 mL) at RT under nitrogen. 5,5'-Diacetyl-2,2'-bithiophene (**2b**)^[21] (0.33 g, 1.3 mmol) was added in portions to this solution and the mixture was stirred at RT overnight. Ethyl acetate (20 mL) was added, and the solution washed with hydrochloric acid (2 M, 10 mL × 2) and water (10 mL). The organic solution was dried over MgSO₄ and concentrated. The residue was filtered and washed with *n*-hexane to afford an orange solid (0.58 g). The crude product was purified by sublimation at 180°C and 10⁻² Torr to provide ligand **3b** as orange crystals (0.48 g, 82%). M.p. 193–194°C; ¹H NMR (600 MHz, CDCl₃): δ = 6.44 (s, 2H), 7.40 (d, *J* = 4.1 Hz, 2H), 7.77 ppm (d, *J* = 4.1 Hz, 2H); IR (KBr): $\tilde{\nu}$ = 1576, 1426, 1263, 1235, 1198, 1155, 1117, 799, 683, 635, 581 cm⁻¹; UV/Vis (MeCN): λ_{max} (ϵ) = 421 nm (45 300 mol⁻¹ dm³ cm⁻¹); MS (70 eV): *m/z* (%): 442 (100) [M]⁺, 373 (93), 331 (31); elemental analysis calcd (%) for C₁₆H₈F₆O₄S₂: C 43.44, H 1.82; found: C 43.45, H 1.66.

Ligand 3c: Obtained as yellow crystals (0.42 g, 75%). M.p. 223.5–224°C; ¹H NMR (600 MHz, CDCl₃): δ = 6.52 (s, 2H), 7.06 (d, *J* = 3.8 Hz, 2H), 7.44 ppm (d, *J* = 3.8 Hz, 2H); IR (KBr): $\tilde{\nu}$ = 1642, 1601, 1561, 1422, 1314, 1263, 1181, 1144, 1103, 1071, 1022, 802, 666 cm⁻¹; UV/Vis (MeCN): λ_{max} (ϵ) = 412 nm (44 600 mol⁻¹ dm³ cm⁻¹); MS (70 eV): *m/z* (%): 410 (100) [M]⁺, 341 (95), 299 (62); elemental analysis calcd (%) for C₁₆H₈F₆O₄: C 46.85, H 1.97; found: C 46.76, H 1.78.

Ligand 3d:^[22] Obtained as yellow crystals (0.35 g, 64%). M.p. 177.5–178°C; ¹H NMR (600 MHz, CDCl₃): δ = 6.62 (s, 2H), 7.78 (d, *J* = 8.6 Hz, 4H), 8.06 ppm (d, *J* = 8.6 Hz, 4H); IR (KBr): $\tilde{\nu}$ = 1601, 1445, 1271, 1213, 1154, 1111, 795, 718, 627, 577 cm⁻¹; UV/Vis (MeCN): λ_{max} (ϵ) = 362 nm (54 300 mol⁻¹ dm³ cm⁻¹); MS (70 eV): *m/z* (%): 431 (96) [M+1]⁺, 362 (100), 319 (54); elemental analysis calcd (%) for C₂₀H₁₂F₆O₄: C 55.83, H 2.81; found: C 55.87, H 2.74.

Synthesis of BF₂ complex 1a: A mixture of ligand **3a** (115 mg, 0.22 mmol) and BF₃·OEt₂ (2.0 mL, 16 mmol) was heated at reflux for 4 h under nitrogen. After removal of excess BF₃·OEt₂ under reduced pressure, the residue was collected by filtration and washed with chloroform and *n*-hexane to afford **1a** as dark purple crystals (117 mg, 86%). Because an elemental analysis revealed that the crystals had sufficient purity, further purification was not performed. ¹H NMR (600 MHz, CDCl₃): δ = 6.74 (s, 2H), 7.48 (d, *J* = 4.6 Hz, 2H), 7.55 (s, 2H), 8.15 ppm (d, *J* = 4.6 Hz, 2H); IR (KBr): $\tilde{\nu}$ = 1603, 1505, 1422, 1356, 1277, 1206, 1032, 802 cm⁻¹; UV/Vis (MeCN): λ_{max} (ϵ) = 517 nm (59 400 mol⁻¹ dm³ cm⁻¹); MS (70 eV): *m/z* (%): 620 (93) [M]⁺, 187 (58), 139 (100); elemental analysis calcd (%) for C₂₀H₈B₂F₁₀O₄S₃: C 38.74, H 1.30; found: C 38.68, H 1.10.

Complexes 1b–e: Similar reaction conditions to that described for **1a** were applied to the synthesis of these complexes. The crude products were sublimed at 215 (**1b,c,e**) or 240°C (**1d**) at 10⁻³ Torr to provide pure products.

Complex 1b: Obtained as red crystals (38 mg, 30%). IR (KBr): $\tilde{\nu}$ = 1595, 1510, 1427, 1350, 1263, 1202, 1038, 953, 822, 681 cm⁻¹; UV/Vis (MeCN): λ_{max} (ϵ) = 488 (61 500), 466 nm (59 900 mol⁻¹ dm³ cm⁻¹); MS (70 eV): *m/z* (%): 538 (100) [M]⁺, 469 (66), 379 (41); elemental analysis calcd (%) for C₁₆H₆B₂F₁₀O₄S₂: C 35.72, H 1.12; found: C 35.75, H 0.86.

Complex 1c: Obtained as orange crystals (56 mg, 47%). IR (KBr): $\tilde{\nu}$ = 1605, 1584, 1524, 1451, 1410, 1370, 1329, 1273, 1217, 1159, 1053, 1026, 972, 820, 679 cm⁻¹; UV/Vis (MeCN): λ_{max} (ϵ) = 482 (74800), 457 nm sh (57900 mol⁻¹ dm³ cm⁻¹); MS (70 eV): m/z (%): 506 (33) [M]⁺, 369 (100); elemental analysis calcd (%) for C₁₆H₆B₂F₁₀O₆: C 37.99, H 1.20; found: C 37.92, H 1.13.

Complex 1d: Obtained as yellow crystals (0.32 g, 86%). ¹H NMR (600 MHz, CDCl₃): δ = 7.06 (s, 2H), 7.92 (d, J = 8.7 Hz, 4H), 8.34 ppm (d, J = 8.7 Hz, 4H); IR (KBr): $\tilde{\nu}$ = 1593, 1350, 1321, 1271, 1206, 1169, 1047, 812 cm⁻¹; UV/Vis (MeCN): λ_{max} (ϵ) = 389 nm (65500 mol⁻¹ dm³ cm⁻¹); MS (70 eV): m/z (%): 526 (100) [M]⁺, 457 (79), 367 (72); elemental analysis calcd (%) for C₂₀H₁₀B₂F₁₀O₄: C 45.68, H 1.92; found: C 45.83, H 1.72.

Complex 1e: Obtained as orange crystals (70 mg, 63%). IR (KBr): $\tilde{\nu}$ = 1580, 1530, 1510, 1427, 1354, 1231, 1204, 1148, 1030 cm⁻¹; UV/Vis (CH₂Cl₂): λ_{max} (ϵ) = 490 nm (50000), 464 nm (57400 mol⁻¹ dm³ cm⁻¹); MS (70 eV): m/z (%): 1040 (100) [M+2]⁺, 1021 (39), 720 (87), 629 (31); elemental analysis calcd (%) for C₂₆H₆B₂F₁₀O₄S₂: C 30.08, H 0.58; found: C 29.98, H 0.55.

X-ray crystallography for 1b: A single crystal was obtained by slow sublimation at 160 °C under nitrogen. Crystal data for **1b**: 0.10 × 0.02 × 0.01 mm; C₁₆H₆B₂F₁₀O₄S₂; M_r = 537.97; orange needle; orthorhombic; space group *Pc2₁b*; a = 4.836(3), b = 12.485(9), c = 31.90(2) Å; V = 1926(2) Å³; Z = 4; ρ_{calcd} = 1.855 g cm⁻³; μ = 0.40 mm⁻¹; $F(000)$ = 1064. Reflection data were collected by using a Rigaku/MSC Mercury CCD diffractometer equipped with a confocal monochromator with MoK α radiation (λ = 0.71070 Å) at 150(1) K. No absorption correction was applied. The structure was solved by direct method using SHELXS97.^[23] All non-hydrogen atoms were refined anisotropically by full-matrix least-squares technique on F^2 by using SHELXL97.^[23] All hydrogen atoms were positioned geometrically and refined by using a riding model. The final values of R_1 = 0.115, GOF = 0.86 and max./min. residual electron density 1.29/−0.56 e Å⁻³ were obtained for 2761 unique reflections [$I > 2\sigma(I)$]. CCDC-763409 contains the supplementary crystallographic data for this paper. These data can be obtained free of charge from The Cambridge Crystallographic Data Centre via www.ccdc.cam.ac.uk/data_request/cif.

OFET fabrication with 1e: A highly doped n⁺-Si wafer was used as substrate. An SiO₂ film (300 nm) grown by thermal oxidation was used as the gate dielectric layer. Source and drain electrodes were photolithographically delineated by evaporating Cr (10 nm)/Au (20 nm). The channel length and width of source-drain contacts were 25 μ m and 294 nm (6 mm × 49), respectively. The substrate was immersed in hexamethyldisilazane at RT overnight. A thin film (70 nm) of **1e** was deposited on the channel region at 90 °C by vacuum evaporation at a rate of 0.02–0.03 nm s⁻¹ under a pressure of 10⁻⁵ Pa. The OFET measurements were performed at RT in a vacuum chamber in the absence of air. The output and transfer characteristics are shown in Figure 6.

Acknowledgements

This work was supported by a Grant-in-Aid for Scientific Research (no. 20550037) from the Ministry of Education, Culture, Sports, Science and Technology, Japan. We thank The Mazda Foundation and ADEKA CORP. for their financial support and Riken Keiki Co. for the measurement of ionization potentials by using AC-3. We thank the Instrument Center of the Institute for Molecular Science for the X-ray crystallography.

- [1] a) Y. Liu, J. Guo, H. Zhang, Y. Wang, *Angew. Chem.* **2002**, *114*, 190–192; *Angew. Chem. Int. Ed.* **2002**, *41*, 182–184; b) H. Zhang, C. Huo, K. Ye, P. Zhang, W. Tian, Y. Wang, *Inorg. Chem.* **2006**, *45*, 2788–2794; c) H. Zhang, C. Huo, J. Zhang, P. Zhang, W. Tian, Y. Wang, *Chem. Commun.* **2006**, 281–283; d) Z. Zhang, H. Bi, Y. Zhang, D. Yao, H. Gao, Y. Fan, H. Zhang, Y. Wang, Y. Wang, Z. Chen, D. Ma, *Inorg. Chem.* **2009**, *48*, 7230–7236.

- [2] a) S.-F. Liu, Q. Wu, H. L. Schmider, H. Aziz, N.-X. Hu, Z. Popović, S. Wang, *J. Am. Chem. Soc.* **2000**, *122*, 3671–3678; b) Q. Liu, M. S. Mudadu, H. Schmider, R. Thummel, Y. Tao, S. Wang, *Organometallics* **2002**, *21*, 4743–4749; c) Q.-D. Liu, M. S. Mudadu, R. Thummel, Y. Tao, S. Wang, *Adv. Funct. Mater.* **2005**, *15*, 143–154.
- [3] H.-Y. Chen, Y. Chi, C.-S. Liu, J.-K. Yu, Y.-M. Cheng, K.-S. Chen, P.-T. Chou, S.-M. Peng, G.-H. Lee, A. J. Carty, S.-J. Yeh, C.-T. Chen, *Adv. Funct. Mater.* **2005**, *15*, 567–574.
- [4] a) S. Kappaun, S. Rentenberger, A. Pogantsch, E. Zojer, K. Mereiter, G. Trimmel, R. Saf, K. C. Möller, F. Stelzer, C. Slugovc, *Chem. Mater.* **2006**, *18*, 3539–3547; b) Y. Cui, Q.-D. Liu, D.-R. Bai, W.-L. Jia, Y. Tao, S. Wang, *Inorg. Chem.* **2005**, *44*, 601–609; c) Q. Wu, M. Esteghamatian, N.-X. Hu, Z. Popovic, G. Enright, Y. Tao, M. D'Iorio, S. Wang, *Chem. Mater.* **2000**, *12*, 79–83; d) S. L. Hellstrom, J. Ugolotti, G. J. P. Britovsek, T. S. Jones, A. J. P. White, *New J. Chem.* **2008**, *32*, 1379–1387; e) Y. Qin, I. Kiburu, S. Shah, F. Jäkle, *Org. Lett.* **2006**, *8*, 5227–5230.
- [5] a) Y. Qin, I. Kiburu, S. Shah, F. Jäkle, *Macromolecules* **2006**, *39*, 9041–9048; b) Y. Nagata, Y. Chujo, *Macromolecules* **2007**, *40*, 6–8; c) Y. Nagata, Y. Chujo, *Macromolecules* **2008**, *41*, 2809–2813; d) Y. Nagata, H. Otaka, Y. Chujo, *Macromolecules* **2008**, *41*, 737–740.
- [6] a) A. Loudet, K. Burgess, *Chem. Rev.* **2007**, *107*, 4891–4932; b) R. Ziessel, G. Ulrich, A. Harriman, *New J. Chem.* **2007**, *31*, 496–501; c) A. Harriman, L. J. Mallon, K. J. Elliot, A. Haefele, G. Ulrich, R. Ziessel, *J. Am. Chem. Soc.* **2009**, *131*, 13375–13386; d) S. Diring, F. Puntoriero, F. Nastasi, S. Campagna, R. Ziessel, *J. Am. Chem. Soc.* **2009**, *131*, 6108–6110; e) T. Rousseau, A. Cravino, T. Bura, G. Ulrich, R. Ziessel, J. Roncali, *Chem. Commun.* **2009**, 1673–1675; f) C. Y. Lee, J. T. Hupp, *Langmuir* **2010**, *26*, 3760–3765.
- [7] a) Z.-N. Sun, H.-L. Wang, F.-Q. Liu, Y. Chen, P. K. H. Tam, D. Yang, *Org. Lett.* **2009**, *11*, 1887–1890; b) Z. Ekmekci, M. D. Yilmaz, E. U. Akkaya, *Org. Lett.* **2008**, *10*, 461–464; c) Z.-N. Sun, F.-Q. Liu, Y. Chen, P. K. H. Tam, D. Yang, *Org. Lett.* **2008**, *10*, 2171–2174; d) A. Palma, M. Tasiar, D. O. Frimannson, T. T. Vu, R. Méallet-Renault, D. F. O'Shea, *Org. Lett.* **2009**, *11*, 3638–3641; e) D. P. Kennedy, C. M. Kormos, S. C. Burdette, *J. Am. Chem. Soc.* **2009**, *131*, 8578–8586.
- [8] a) F. Camerel, L. Bonardi, M. Schmutz, R. Ziessel, *J. Am. Chem. Soc.* **2006**, *128*, 4548–4549; b) A. Nagai, J. Miyake, K. Kokado, Y. Nagata, Y. Chujo, *J. Am. Chem. Soc.* **2008**, *130*, 15276–15278.
- [9] a) S. Erten-Ela, M. D. Yilmaz, B. Icli, Y. Dede, S. Icli, E. U. Akkaya, *Org. Lett.* **2008**, *10*, 3299–3302; b) S. Hattori, K. Ohkubo, Y. Urano, H. Sunahara, T. Nagano, Y. Wada, N. V. Tkachenko, H. Lemmetyinen, S. Fukuzumi, *J. Phys. Chem. B* **2005**, *109*, 15368–15375; c) D. Kumaresan, R. P. Thummel, T. Bura, G. Ulrich, R. Ziessel, *Chem. Eur. J.* **2009**, *15*, 6335–6339.
- [10] a) Y. Inokuma, J. H. Kwon, T. K. Ahn, M.-C. Yoo, D. Kim, A. Osuka, *Angew. Chem.* **2006**, *118*, 975–978; *Angew. Chem. Int. Ed.* **2006**, *45*, 961–964; b) N. Kobayashi, Y. Takeuchi, A. Matsuda, *Angew. Chem.* **2007**, *119*, 772–774; *Angew. Chem. Int. Ed.* **2007**, *46*, 758–760; c) Y. Takeuchi, A. Matsuda, N. Kobayashi, *J. Am. Chem. Soc.* **2007**, *129*, 8271–8281; d) Y. Inokuma, Z. S. Yoon, D. Kim, A. Osuka, *J. Am. Chem. Soc.* **2007**, *129*, 4747–4761; e) Y. Inokuma, S. Easwaramoorthi, Z. S. Yoon, D. Kim, A. Osuka, *J. Am. Chem. Soc.* **2008**, *130*, 12234–12235; f) Y. Inokuma, A. Osuka, *Org. Lett.* **2008**, *10*, 5561–5564; g) J.-Y. Liu, H.-S. Yeung, W. Xu, X. Li, D. K. P. Ng, *Org. Lett.* **2008**, *10*, 5421–5424.
- [11] a) H. Maeda, Y. Haketa, T. Nakanishi, *J. Am. Chem. Soc.* **2007**, *129*, 13661–13674; b) H. Maeda, Y. Kusunose, *Chem. Eur. J.* **2005**, *11*, 5661–5666; c) H. Maeda, Y. Mihashi, Y. Haketa, *Org. Lett.* **2008**, *10*, 3179–3182.
- [12] a) A. Nagai, K. Kokado, Y. Nagata, M. Arita, Y. Chujo, *J. Org. Chem.* **2008**, *73*, 8605–8607; b) A. Nagai, K. Kokado, Y. Nagata, Y. Chujo, *Macromolecules* **2008**, *41*, 8295–8298.
- [13] E. Cogné-Laage, J.-F. Allemand, O. Ruel, J.-B. Baudin, V. Croquette, M. Blanchard-Desce, L. Jullien, *Chem. Eur. J.* **2004**, *10*, 1445–1455.
- [14] K. Ono, K. Yoshikawa, Y. Tsuji, H. Yamaguchi, R. Uozumi, M. Tomura, K. Taga, K. Saito, *Tetrahedron* **2007**, *63*, 9354–9358.

- [15] Y. Sun, D. Rohde, Y. Liu, L. Wan, Y. Wang, W. Wu, C. Di, G. Yu, D. Zhu, *J. Mater. Chem.* **2006**, *16*, 4499–4503.
- [16] a) K. Ono, H. Yamaguchi, K. Taga, K. Saito, J. Nishida, Y. Yamashita, *Org. Lett.* **2009**, *11*, 149–152; b) K. Ono, J. Hashizume, H. Yamaguchi, M. Tomura, J. Nishida, Y. Yamashita, *Org. Lett.* **2009**, *11*, 4326–4329.
- [17] a) M.-H. Yoon, S. A. DiBenedetto, A. Facchetti, T. J. Marks, *J. Am. Chem. Soc.* **2005**, *127*, 1348–1349; b) M.-H. Yoon, S. A. DiBenedetto, M. T. Russell, A. Facchetti, T. J. Marks, *Chem. Mater.* **2007**, *19*, 4864–4881; c) M.-H. Yoon, A. Facchetti, C. E. Stern, T. J. Marks, *J. Am. Chem. Soc.* **2006**, *128*, 5792–5801; d) A. Facchetti, M. Mushrush, M.-H. Yoon, G. R. Hutchison, M. A. Ratner, T. J. Marks, *J. Am. Chem. Soc.* **2004**, *126*, 13859–13874; e) J. A. Letizia, A. Facchetti, C. L. Stern, M. A. Ratner, T. J. Marks, *J. Am. Chem. Soc.* **2005**, *127*, 13476–13477; f) Y. Ie, Y. Umemoto, M. Okabe, T. Kusunoki, K. Nakayama, Y.-J. Pu, J. Kido, H. Tada, Y. Aso, *Org. Lett.* **2008**, *10*, 833–836; g) Y. Ie, M. Nitani, M. Ishikawa, K. Nakayama, H. Tada, T. Kaneda, Y. Aso, *Org. Lett.* **2007**, *9*, 2115–2118; h) S. Ando, J. Nishida, H. Tada, Y. Inoue, S. Tokito, Y. Yamashita, *J. Am. Chem. Soc.* **2005**, *127*, 5336–5337; i) Y. Ie, M. Nitani, T. Uemura, Y. Tominari, J. Takeya, Y. Honsho, A. Saeki, S. Seki, Y. Aso, *J. Phys. Chem. C* **2009**, *113*, 17189–17193; j) S. Handa, E. Miyazaki, K. Takimiya, Y. Kunugi, *J. Am. Chem. Soc.* **2007**, *129*, 11684–11685.
- [18] Gaussian 03, Revision D.02, M. J. Frisch, G. W. Trucks, H. B. Schlegel, G. E. Scuseria, M. A. Robb, J. R. Cheeseman, J. A. Montgomery, Jr., T. Vreven, K. N. Kudin, J. C. Burant, J. M. Millam, S. S. Iyengar, J. Tomasi, V. Barone, B. Mennucci, M. Cossi, G. Scalmani, N. Rega, G. A. Petersson, H. Nakatsuji, M. Hada, M. Ehara, K. Toyota, R. Fukuda, J. Hasegawa, M. Ishida, T. Nakajima, Y. Honda, O. Kitao, H. Nakai, M. Klene, X. Li, J. E. Knox, H. P. Hratchian, J. B. Cross, V. Bakken, C. Adamo, J. Jaramillo, R. Gomperts, R. E. Stratmann, O. Yazyev, A. J. Austin, R. Cammi, C. Pomelli, J. W. Ochterski, P. Y. Ayala, K. Morokuma, G. A. Voth, P. Salvador, J. J. Dannenberg, V. G. Zakrzewski, S. Dapprich, A. D. Daniels, M. C. Strain, O. Farkas, D. K. Malick, A. D. Rabuck, K. Raghavachari, J. B. Foresman, J. V. Ortiz, Q. Cui, A. G. Baboul, S. Clifford, J. Cioslowski, B. B. Stefanov, G. Liu, A. Liashenko, P. Piskorz, I. Komaromi, R. L. Martin, D. J. Fox, T. Keith, M. A. Al-Laham, C. Y. Peng, A. Nanayakkara, M. Challacombe, P. M. W. Gill, B. Johnson, W. Chen, M. W. Wong, C. Gonzalez, J. A. Pople, Gaussian Inc., Wallingford, CT, **2004**.
- [19] The n-type semiconducting performance in the bottom-contact OFET is comparable to those of other oligothiophene derivatives.^[17]
- [20] A. R. Sørensen, L. Overgaard, I. Johannsen, *Synth. Met.* **1993**, *55*, 1626–1631.
- [21] J. Hassan, C. Gozzi, M. Lemaire, *C. R. Acad. Sci. Ser. II: Chim.* **2000**, *3*, 517–521.
- [22] J. Yuan, S. Sueda, R. Somazawa, K. Matsumoto, K. Matsumoto, *Chem. Lett.* **2003**, *32*, 492–493.
- [23] G. M. Sheldrick, *Acta Crystallogr. Sect. A* **2008**, *64*, 112–122.

Received: May 4, 2010

Published online: October 11, 2010